Numerical Evaluation of Scour-Hole Formation Procedures in Centrifuge Modelling for Laterally Loaded Monopiles

Ben WU
Department of Civil and Environmental Engineering, National University of Singapore, Singapore, benwu@u.nus.edu
Siau Chen Chian
Department of Civil and Environmental Engineering, National University of Singapore, Singapore, sc.chian@nus.edu.sg

ABSTRACT: In centrifuge model tests involving the investigation of scour on lateral bearing capacity of monopiles, the scour hole is often pre-excavated at 1g, followed by acceleration to the target Ng before lateral loading is applied. However, this preparation sequence may alter the initial stress state and stress path during scour hole formation, potentially compromising the extension of test results to prototype conditions. This study establishes two comparative simulation schemes using PLAXIS at the centrifuge model scale: (A) 1g scouring → acceleration to Ng → lateral loading, and (B) acceleration to Ng → Ng scouring → lateral loading. The acceleration process is simulated via incremental self-weight multipliers ∑Mweight. The results demonstrate quantifiable discrepancies between the two schemes in terms of pile-top load-displacement response, ultimate soil resistance, and initial stiffness. Scheme A tends to underestimate the lateral bearing capacity of the monopile compared to Scheme B. These differences are primarily attributed to the unloading stress history during the scouring stage and the subsequent soil stress redistribution around the monopile. This research provides a valuable benchmark for assessing the applicability of simplified centrifuge scour test procedures and facilitates the integration of numerical and physical modelling.

KEYWORDS: Monopile, bearing capacity, scour, centrifuge modelling, FEM.

1 INTRODUCTION

Local scour is prone around the monopile foundation of offshore wind turbines under the impact of waves and currents. The formation of scour holes not only changes the geometric confinement of the soil surrounding the monopile, but also induces stress redistribution and potential changes in soil properties around the monopile, thereby reducing the lateral bearing capacity and lateral stiffness of the monopile (Guen et al., 2022). Numerous studies have been conducted using laboratory tests (Liu et al., 200; Huang et al., 2025; Tao et al., 2025), centrifuge modelling (Qi et al., 2016; Li et al., 2021; Wang et al., 2025), and numerical simulations (Dai et al., 2021; Wang et al., 2025; Wu et al., 2026) for the mechanical mechanism of scour influence and the prediction of monopile bearing capacity. Among these, centrifuge tests enable observation of complex soil-pile interaction and the evolution of deformation and failure under stress-similar conditions, providing critical physical evidence for understanding the lateral response of monopiles in scoured seabed.

Due to limitations associated with reproducing the scour process, experimental operability, and cost, many existing centrifuge studies adopt a simplified preparation procedure, which excavates the scour hole under 1g, ramps up to the target acceleration (Ng), and then applies lateral loading. This procedure assumes that the scour hole pre-excavated at 1g can represent the initial state after the formation of scour hole at the target stress level. In reality, scouring is an unloading procedure. The stress level and stress path at the time of excavation may influence the stress release range, plastic strain accumulation, and the soil-pile interface contact condition near the scour hole, thereby causing bias in the response of soil-pile interaction under lateral loading.

To evaluate the influence of this simplification, this study adopts an integrated numerical-physical framework and develops equivalent centrifuge models with two scour-hole preparation sequences: Scheme A (scour at 1g → ramp to Ng → load) and Scheme B (ramp to Ng → scour at Ng → load). By comparing key response results such as load-displacement curves and soil-pile interaction (*p*-*y* curves), and by further examining differences in the soil stress-field distributions, the bias induced by the scour-hole preparation sequence is quantified.

2 NUMERICAL ANALYSIS

2.1 Overview of centrifuge modelling

To investigate the influence of scour on the lateral response of monopile, Li et al. (2021) conducted a 100g centrifuge test series on a laterally loaded open-ended tubular monopile in sand. The model pile had D = 18 mm and embedment L = 90 mm (L/D = 5), with lateral load applied at an eccentricity of e = 8D above the original sand surface. The schematic diagram and set up of centrifuge modelling are shown in Figure 1.

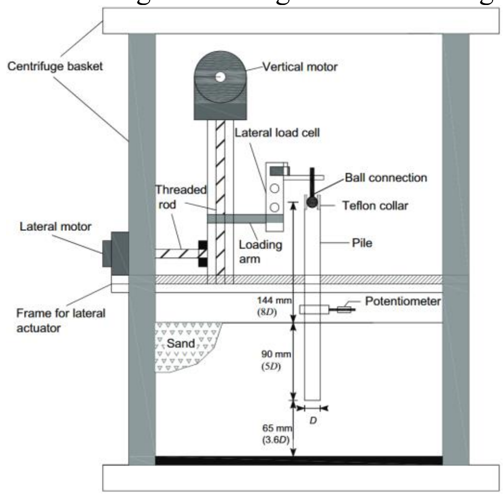

(a) schematic diagram

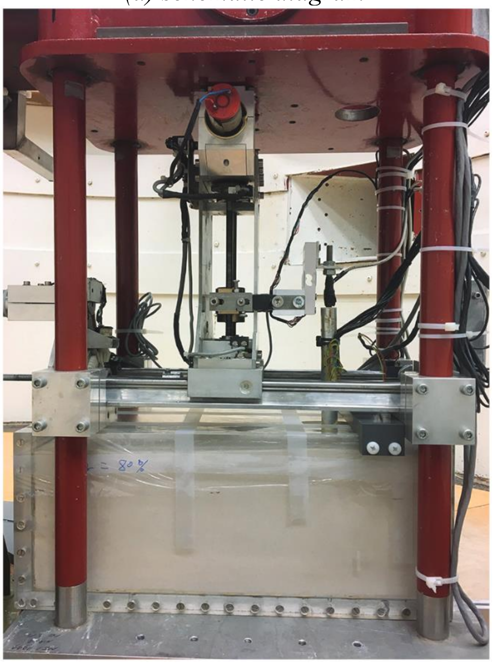

(b) Centrifuge modelling

Figure 1. Two-dimensional loading actuator and pile testing set-up

The test programme comprised 10 monotonic lateral cases: a single no-scour reference and nine scour cases (3 shapes × 3 depths). For scour testing, the representative local wide scour is selected as the simulation scenario in this study, including three different scour depths S_d = 1.0D, 1.5D, 2.0D, as shown in Figure 2.

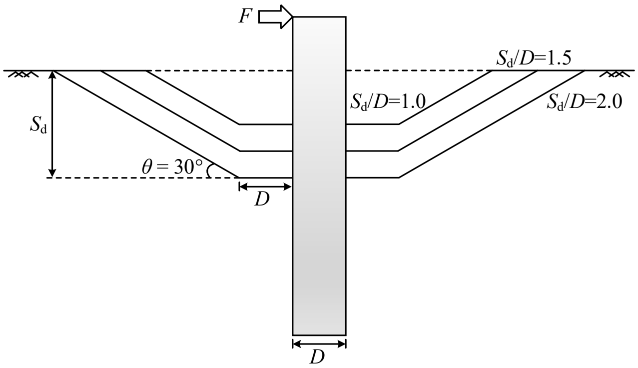

Figure 2. Simulation cases

2.2 FEM modelling

The commercial finite-element software PLAXIS 3D is employed to establish the soil-pile-scour model, as shown in Figure 3. The scour hole is modelled as an inverted frustum, consistent with the geometry assumed in the centrifuge tests. S_d, S_{wb}, S_{wt}, and θ denote the depth, bottom width, top width, and slope angle of the scour hole, respectively. Based on the geometric relationship, S_{wt} can be derived from the other three parameters as follows:

$$S_{wt} = S_{wb} + S_d \cot\theta \quad (1)$$

Due to the symmetry of the scour hole shape along the loading direction, only half of the model is established. The soil is modelled using solid elements, with a computational domain of 8(S_{wt} + D/2) × 4(S_{wt} + D/2) × 2.5L. The monopile is simulated using shell elements. Its dimensions, including diameter, loading height, embedment depth, and wall thickness, are identical to those used in the centrifuge tests. To capture the soil-pile interaction, interface elements are implemented between the soil and pile, with a strength reduction factor R_{inter} = 0.7.

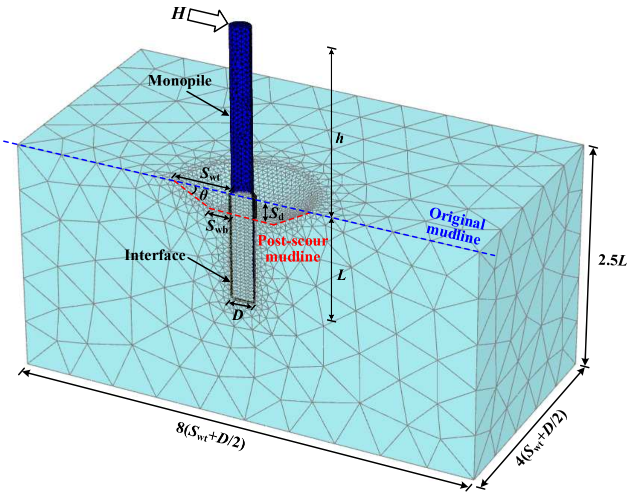

Figure 3. FEM modelling

In selecting a soil constitutive model, two essential factors should be simultaneously considered: the stress-dependency of sand stiffness and the loading history. Centrifuge acceleration to Ng aims to replicate the high-stress levels of the prototype. The soil modulus will vary significantly with these stress levels. Furthermore, scour and loading are essentially processes of unloading and reloading. The model should reliably predict the rebound and reloading stiffness. Based on these considerations, the Hardening Soil model with Small-strain stiffness (HSS model) is selected to simulate the stress-strain behavior of soil. Beyond the aforementioned factors, HSS model also accounts for the degradation of small-strain shear modulus with increasing shear strain, thereby providing a more reasonable estimation of monopile responses.

The parameter values for the HSS model refer to Li et al. (2021), as listed in Table 1. These parameters are derived from Geba silica sand used in centrifuge tests and have been validated through experimental data.

Table 1. Simulation parameters

Parameter	Value	Parameter	Value
γ/(kN/m^2)	15.6	υ_{ur}	0.2
c/(kPa)	0.1	p^{ref}/(kPa)	100
φ/(°)	34	K_0	0.44
ψ/(°)	4	R_f	0.9
E_{50}^{re}/(MPa)	41	G_0^{ref}/(MPa)	95.7
E_{oed}^{ref}/(MPa)	21	$\gamma_{0.7}$	0.19×10^{-3}
E_{ur}^{ref}/(MPa)	123	E/(GPa)	210
M	0.5	υ	0.3

2.3 Simulation procedure

To simulate the centrifuge acceleration process, the gravity multiplier $\sum M_{weight}$ in PLAXIS is utilized to amplify the self-weight incrementally. By step-wisely increasing $\sum M_{weight}$ from 1g to Ng, the model achieves an effective stress level equivalent to a centrifuge field of N times gravity while maintaining a constant geometric scale. This approach effectively realises the equivalent simulation of centrifuge acceleration. For the reference centrifuge test in this study, the final acceleration is 100g.

Two simulation schemes are designed to evaluate the impact of the formation sequence of scour hole, as shown in Figure 4:

a) Scheme A: After establishing the initial 1g stress field, the scour hole is first excavated by removing soil elements, and static equilibrium is achieved at 1g. Subsequently, $\sum M_{weight}$ is incrementally increased from 1 to 100 to complete the acceleration process and reach equilibrium at 100g. Finally, lateral loading is applied at 100g to obtain the load-displacement response.

b) Scheme B: Following the establishment of the 1g stress field, the soil stress is first increased to the 100g level and allowed to reach equilibrium. The scour hole is then excavated under the 100g condition. Finally, lateral loads are applied until the monopile reached failure.

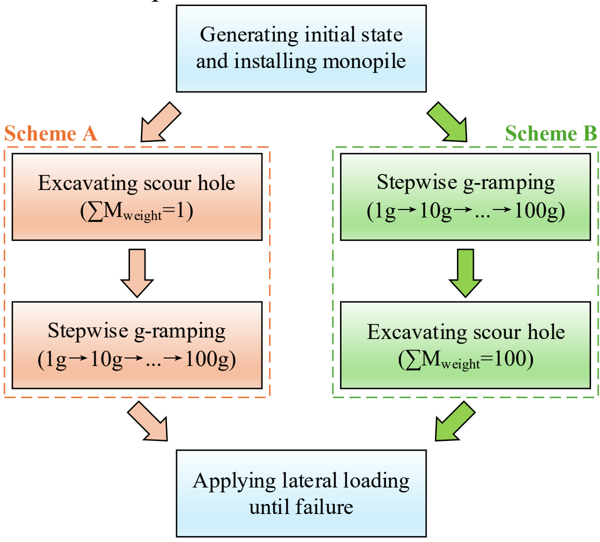

Figure 4. Simulation procedure of different formation sequences of scour hole

3 RESULTS AND DISCUSSIONS

Figure 5 illustrates the dimensionless lateral load-displacement responses of the monopile head under two scour hole preparation schemes across different scour depth ratios S_d/D. Overall, as S_d/D increases from 1.0 to 2.0, the curves shift downward significantly, indicating that increased scour depth substantially reduces the lateral bearing capacity and stiffness of monopile. A comparison of the two schemes reveals that, under identical S_d/D conditions, Scheme B yields a significantly higher lateral capacity and a steeper initial slope than Scheme A, reflecting higher initial lateral stiffness. This suggests that the stress level and stress path during scour hole formation alter the initial state of the soil around the monopile. Pre-excavating the scour hole at 1g (Scheme A) is equivalent to unloading at a low confining pressure; the subsequent stress history of increasing g-level before loading is more likely to cause soil stress relaxation and stiffness degradation, resulting in lower mobilization of soil resistance. In contrast, excavating at 100g (Scheme B) forms the scour hole under a higher stress level, maintaining stronger confinement before loading, thus exhibiting higher capacity and stiffness.

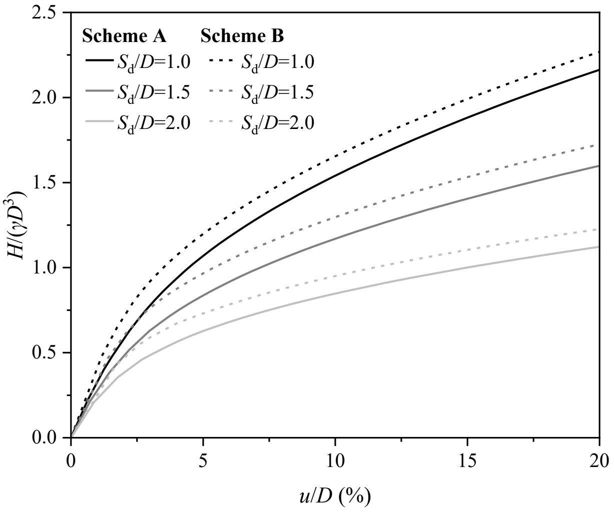

Figure 5. Influence on lateral loading-displacement curve

The distribution of ultimate soil resistance is shown in Figure 6. The soil resistance level for Scheme B is generally higher than that of Scheme A, with the discrepancy primarily concentrated between the positive peak value and the zero-point, rather than in the shallow regions closest to the scour hole. This is attributed to the low stress levels and weak confinement in shallow soils, where mobilizable resistance is limited. Conversely, the peak-to-zero interval maintains continuous soil-pile contact and bears the primary lateral reaction, making it more sensitive to the preparation scheme of scour.

To eliminate scale effects induced by varying scour depths, a dimensionless relative depth z', is defined. It is defined as the ratio of the distance from any point below the scour hole to the scour base relative to the effective embedment depth of the pile.

$$z' = \frac{z - S_d}{L - S_d} \tag{2}$$

The dimensionless ultimate soil resistance distribution is shown in Figure 7. The curves for different scour depths converge, suggesting that the ultimate soil resistance is primarily governed by relative depth z' rather than absolute depth z. Furthermore, the divergence between the two preparation schemes becomes more pronounced, indicating that simplifying the scour hole preparation sequence (as in Scheme A) tends to underestimate the bearing capacity of the monopile pile.

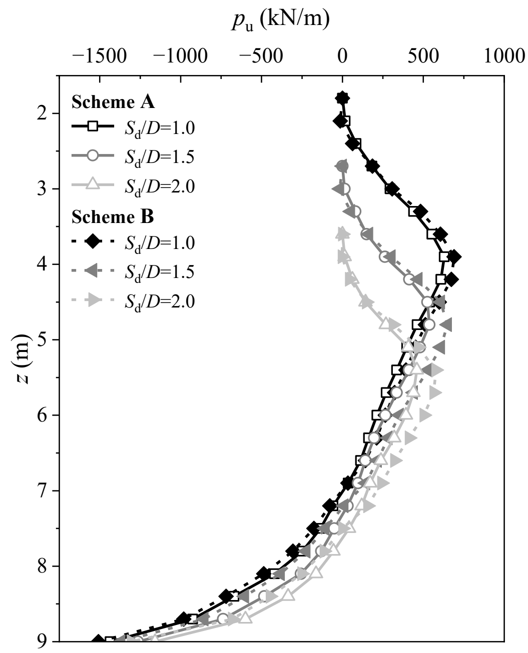

Figure 6. Influence on the distribution of soil resistance with absolute depth z

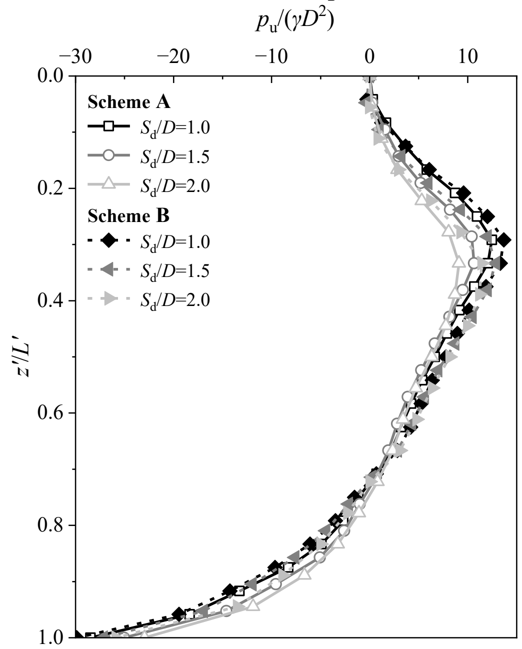

Figure 7. Influence on the distribution of soil resistance with relative depth z'

A comparison of *p-y* curves at absolute depth *z* is shown in Figure 8. At *z* = 4 m, Scheme B exhibits a higher ultimate soil resistance and initial slope (i.e., initial foundation reaction modulus), implying stronger lateral confinement at the same displacement level. Notably, when S_d/D = 2.0, *z* = 4 m is near the scour base where *p-y* curves approach zero, rendering them insensitive to the preparation scheme. More significant differences are observed at *z* = 5 m, as shown in Figure 8(b). Across all three scour depth ratios, *z* = 5 m falls within the peak-to-zero interval of soil resistance, where the preparation scheme significantly impacts *p-y* curve characteristics.

Scheme B curves consistently envelop those of Scheme A, with substantial differences in the ultimate soil resistance, aligning with the previously discussed distribution patterns.

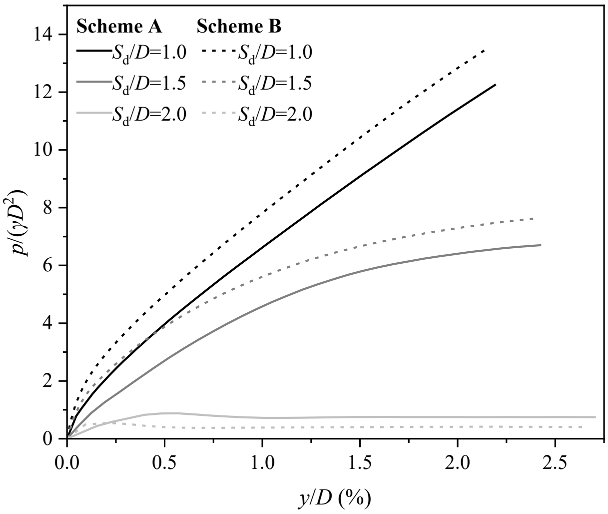

(a) z = 4m

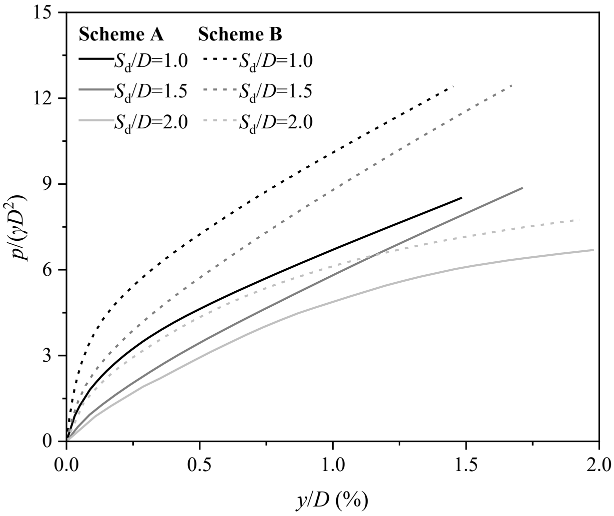

(b) z = 5m

Figure 8. Influence on p-y curve with different absolute depths

Comparisons of *p-y* curves based on relative depth z' are shown in Figure 9. It reveals that while ultimate resistance still varies significantly across depths, the initial slopes for each scheme remain essentially identical. This demonstrates that the initial subgrade reaction modulus is also primarily influenced by relative depth rather than absolute depth. Furthermore, the narrowing gap between the two schemes suggests that relative depth is a rational index for describing soil-pile interaction under scouring conditions.

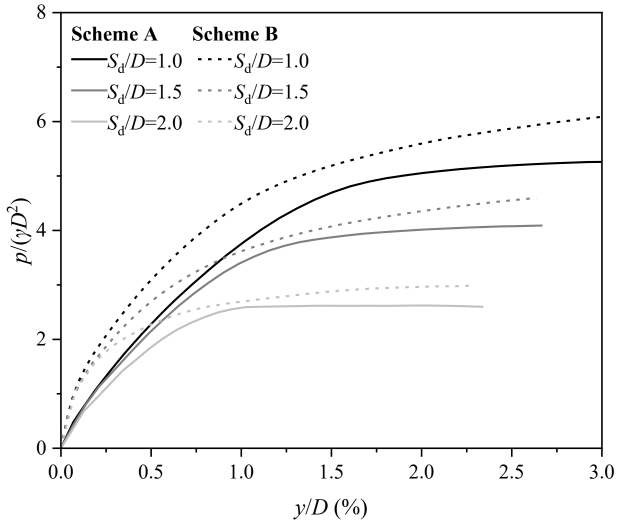

(a) z' = 1/6

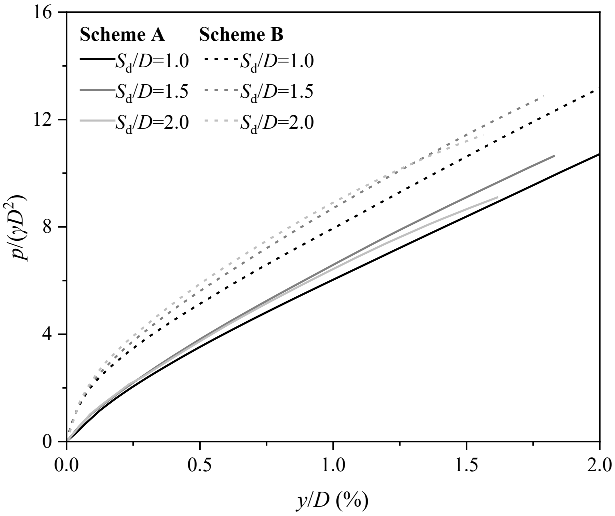

(b) z' = 1/3

Figure 9. Influence on p-y curve with different normalized depths z'

4 CONCLUSIONS

This study compared two scour hole preparation sequences using PLAXIS at the centrifuge model scale: pre-excavation at 1g followed by acceleration to 100g (Scheme A), and excavation performed after reaching 100g (Scheme B). The results indicate that Scheme B consistently exhibits higher dimensionless lateral capacity and initial stiffness. Comparative analyses of *p-y* curves and ultimate soil resistance reveal that the discrepancies are primarily concentrated in the main contribution zone below the scour hole base. These differences originate from the distinct unloading-reloading paths governed by the stress levels at the time of excavation. Pre-excavation at 1g is more prone to inducing near-field stiffness degradation, thereby weakening the subsequent mobilization of soil resistance. Based on these findings, it is recommended that numerical procedures involving simplified 1g pre-excavation be carefully calibrated. Where necessary, an excavation scheme at the N-g level should be adopted to ensure the fidelity of the simulation.

ACKNOWLEDGEMENTS

The authors are grateful for the Ph.D. scholarship support to the first author, provided by the Singapore Ministry of Education (MOE).

REFERENCES

Dai, S., Han, B., Wang, B., Luo, J., and He, B. (2021). Influence of soil scour on lateral behavior of large-diameter offshore wind-turbine monopile and corresponding scour monitoring method. *Ocean Engineering*, 239, 109809.

Guan, D. W., Xie, Y. X., Yao, Z. S., Chiew, Y. M., Zhang, J. S., and Zheng, J. H. (2022). Local scour at offshore windfarm monopile foundations: A review. *Water Science and Engineering*, 15(1), 29-39.

Huang, K., Wu, X., and Lin, Z. (2025). An advanced laboratorial measurement technique of scour topography based on the fusion method for 3D reconstruction. *Journal of Ocean Engineering and Science*, 10(3), 322-329.

Li, Q., Askarinejad, A., and Gavin, K. (2021). Impact of scour on lateral resistance of wind turbine monopiles: an experimental study. *Canadian Geotechnical Journal*, *58*(11), 1770-1782.

Li, Q., Wang, X., Gavin, K., Jiang, S., Diao, H., Wang, M., and Wang, K. (2024). Scour Effect on the Lateral Bearing Behaviour of Monopiles Considering Different Slenderness Ratios. *Water*, 16(2), 226.

Liu, X., Chen, X., Wang, L., Zhang, F., Zhang, X., and Wang, Y. (2022). Investigation on the scour properties of pile under the current considering the geomechanical parameters of seabed: Time scale. *Ocean Engineering*, 262, 112175.

Qi, W. G., Gao, F. P., Randolph, M. F., and Lehane, B. M. (2016). Scour effects on p–y curves for shallowly embedded piles in sand. *Géotechnique*, 66(8), 648-660.

Tao, G., Zhao, X., Hou, Y., Huang, Z., Zhang, S., and Lu, J. (2025). Experimental investigation on scour characteristics and predictive model of monopile foundations under breaking waves. *Coastal Engineering*, 104764.

Wang, Z., Zhou, H., Franza, A., and Liu, H. (2022). Numerical evaluation of scour effects on lateral behavior of pile groups in clay. *Computers and Geotechnics*, 150, 104913.

Wang, Z., Zhou, H., and Sheil, B. (2025). Effects of scour on the lateral response of piles in sand: centrifuge tests and numerical investigation. *Acta Geotechnica*, 1-20.

Wu, B., and Chian, S. C. (2026). Improved py curve modeling for large-diameter monopiles in asymmetric scour conditions in sandy soils. *Computers and Geotechnics*, *192*, 107880.